Journal of Catalysis 272 (2010) 101–108

Contents lists available at ScienceDirect

Journal of Catalysis

journal homepage: www.elsevier.com/locate/jcat

Dehydrogenation of propane over In_2O_3–Al_2O_3 mixed oxide in the presence of carbon dioxide

Miao Chen, Jie Xu, Yong Cao *, He-Yong He, Kang-Nian Fan, Ji-Hua Zhuang **

Department of Chemistry, Shanghai Key Laboratory of Molecular Catalysis and Innovative Materials, Fudan University, Shanghai 200433, PR China

ARTICLE INFO

Article history:
Received 16 December 2009
Revised 3 March 2010
Accepted 5 March 2010
Available online 3 April 2010

Keywords:
Propane
Propylene
Dehydrogenation
In_2O_3–Al_2O_3
Carbon dioxide
In^0

ABSTRACT

Dehydrogenation of propane (PDH) to propylene in the presence of CO_2 was performed over binary In_2O_3–Al_2O_3 mixed oxides prepared by alcoholic coprecipitation. Synergistic effect of different composition on the catalytic performance has been observed. Characterization by X-ray diffraction and X-ray photoelectron spectroscopy revealed that the combination of the two components can result in significant modification in the surface properties and bulk dispersion of the In_2O_3 phase, which in turn leads to a higher reducibility of the In–Al–O composite. A correlation between the temperature-programmed reduction data and the PDH activity for In_2O_3–Al_2O_3 revealed that the creation of surface metallic indium species during the reaction is crucial for the dehydrogenation performance. The promoting effect of CO_2 on the yield of propylene has been attributed to a facilitation of simple dehydrogenation by its coupling with the reverse water gas shift reaction based on the results from temperature-programmed reaction of CO_2 with H_2.

1. Introduction

Dehydrogenation of light alkanes, such as ethane and propane, into the corresponding alkenes has attracted significant attention since the alkenes constitute an important and versatile class of intermediates in the chemical industry [1,2]. At present, propylene is typically obtained by catalytic dehydrogenation of propane (PDH) [3,4] and as a by-product of steam cracking or a fluidized catalytic cracking (FCC) of naphtha. UOP and AAB Lummus Global, two of the world leaders of catalytic dehydrogenation technology, have licensed eight commercial process units [5], which currently can provide propylene with an aggregate capacity of about 2.1 million metric tons per year. Dehydrogenation of propane, however, is an equilibrium-limited and endothermic reaction [6,7]. For thermodynamics reasons, significant yield of alkene requires operation at relatively high temperatures and thus high-energy costs. Moreover, such process conditions favor undesired thermal cracking reactions to lighter hydrocarbons and notoriously rapid catalyst deactivation due to coke formation [8,9].

An alternative to this process is the oxidative dehydrogenation (ODH) of propane by molecular oxygen [10,11], which has attracted increasing attention due to its higher efficiency of using light alkane resource with minimum energy consumption when compared to the conventional direct dehydrogenation. The ODH gives the following benefits: the reaction is irreversible and exothermic; process can be carried out at lower temperatures without carbon deposition deactivating the catalyst [12–14]. However, using oxygen as an oxidant brings several problems to the reaction [15], such as flammability, necessity of heat removal and deep oxidation, which reduces the process selectivity due to the production of undesired carbon oxides [16] and is hard to control. Therefore, it is expected that replacing oxygen in the ODH reactions by soft oxidants, such as N_2O and CO_2 [17–20], will suppress these disadvantages.

Over the last decade, there has been a growing interest in the use of CO_2 as a milder and safer oxidant in the ODH of propane [6,7,16,20–26]. It is worth noting that the dehydrogenation of propane in the presence of CO_2 can proceed by two different reaction pathways. The first is a direct process, in which CO_2 promotes the dehydrogenation through re-oxidizing the catalyst surface as reduced by propane. This one-step pathway is in agreement with the Mars–Van Krevelen mechanism [16,22,24]. The second one, known as a two-step pathway, is a simple dehydrogenation followed by the reverse water gas shift (RWGS) reaction [7,25,26]. In this case, CO_2 removes hydrogen from the reaction system and releases the thermodynamic limitation of equilibrium. Many results indicate that propylene is formed by both presented mechanisms [20]. Moreover, in the dehydrogenation process, carbon dioxide can act as a diluent [27], which delivers the required heat and reduces coking of catalyst by coke gasification.

To date, the catalysts suggested for propane dehydrogenation with CO_2 are mainly based on supported (transition) metal oxides

* Corresponding author. Fax: +86 21 65643774.
** Corresponding author. Fax: +86 21 65643774.
E-mail addresses: yongcao@fudan.edu.cn (Y. Cao), jihuaz@fudan.edu.cn (J.-H. Zhuang).

0021-9517/$ - see front matter © 2010 Elsevier Inc. All rights reserved.
doi:10.1016/j.jcat.2010.03.007

that allow effective hydrocarbon activation at temperatures significantly lower than conventional dehydrogenation process. Among all the studied catalysts, supported gallium oxides have recently been recognized as one of the most promising materials due to their excellent catalytic efficiency as compared to conventional Cr_2O_3- or Pt-based systems [7,28–33]. One critical limitation associated with the Ga_2O_3-catalyzed PDH process, however, is the drastic deactivation during a few hours on stream [29,30]. Very recently, we have demonstrated that Ga_2O_3–Al_2O_3 mixed oxides are highly active and stable catalysts for PDH in the presence of CO_2 [25,26]. The superior performance of the Ga_2O_3–Al_2O_3 system has been attributed to the formation of gallia-alumina solid solution between Ga_2O_3 and Al_2O_3 [26], which allows the favorable creation of a high abundance of coordinatively unsaturated surface Ga^{3+} sites with weak Lewis acidity. However, the development of new improved catalytic system exhibiting desirable stability and activity still remains a major challenge.

In continuation of our interest in exploring the applications of mixed oxides containing group III elements (Al, Ga and In) in propane dehydrogenation [25,26], herein, we report for the first time the use of In–Al mixed oxide as a new efficient catalyst in the dehydrogenation of propane to prepare propylene. In_2O_3–Al_2O_3 mixed oxides, previously established as an excellent system for selective catalytic reduction (SCR) of NO_x owing to its unique low-temperature redox properties [34–38], have shown to be particularly efficient for PDH in the presence of CO_2. Our results have shown that the creation and maintenance of the catalytically active metallic indium species in optimal surface concentration is indispensable for an efficient dehydrogenation of propane.

2. Experimental

2.1. Catalyst preparation

A series of mixed In_2O_3–Al_2O_3 oxide catalysts with various compositions as well as the simple oxide of Al_2O_3 and In_2O_3 were prepared through a previously developed alcoholic coprecipitation pathway [39]. In a typical synthesis, concentrated aqueous ammonia and ethanol (50:50 in volume) was added dropwise to the ethanol solution of indium nitrate hydrate ($In(NO_3)_3{\cdot}5H_2O$, Aldrich, 99.99%) and aluminum nitrate hydrate ($Al(NO_3)_3{\cdot}9H_2O$, Fluka, 99.9%) with different In:Al molar ratio until no more precipitation occurred (pH = 8.5). The resulting gel was quickly filtered and washed by ethanol, dried at 373 K overnight, and finally calcined at 873 K for 6 h. The final catalyst is denoted as In–Al-*n* hereinafter where *n* represents the mole percentage of In_2O_3.

2.2. Catalyst characterization

The BET-specific surface areas of the samples were determined by adsorption–desorption of nitrogen at liquid nitrogen temperature, using a Micromeritics TriStar 3000 equipment. The X-ray powder diffraction (XRD) of the catalysts was carried out on a Bruker D8Advance X-ray diffractometer using nickel-filtered Cu Kα radiation at 40 kV and 20 mA. The acidic and basic properties of each catalyst were characterized by temperature-programmed desorption (TPD) of NH_3 and CO_2, respectively [26]. In a typical experiment for TPD studies, about 200 mg of the oven-dried sample (dried at 383 K overnight) was placed in a U-shaped quartz sample tube. NH_3 (or CO_2) was saturated at 413 K after pre-treatment at 773 K in a He stream. The NH_3 (or CO_2) desorbed was determined by gas chromatography at temperatures from 413 to 873 K at a ramp rate of 10 K min^{-1} and subsequently maintained at 873 for 20 min.

X-ray photoelectron spectroscopy (XPS) data were recorded on a Perkin Elmer PHI 5000C ESCA system with Mg Kα excitation line ($h\nu$ = 1253.6 eV). The binding energies (BE) were referenced to the C 1s peak of contaminant carbon at 284.6 eV with an uncertainty of ±0.2 eV. Elemental analysis was performed using ion-coupled plasma (ICP) atomic emission spectroscopy on a Thermo Electron IRIS Intrepid II XSP spectrometer. Temperature-programmed reduction (TPR) results were obtained on a homemade apparatus loaded with 20 mg of catalyst. The samples were pretreated in flowing nitrogen at 773 K for 1 h. After cooled to room temperature, the samples were subsequently contacted with an H_2/Ar mixture (H_2/Ar molar ratio of 5/95 and a total flow of 40 mL min^{-1}) and heated at a rate of 5 K min^{-1}, to a final temperature of 1073 K. The H_2 consumption was monitored by an on-line thermal conductivity detector. Since water is produced during reduction, the gas exiting from the reactor was passed through a cold trap before entering the thermal conductivity detector.

2.3. Activity measurement

Catalytic tests were performed in a fixed-bed flow microreactor at atmospheric pressure, and the catalyst amount was 200 mg. Nitrogen was used as the carrier gas at a flow rate of 10 mL min^{-1}. The catalysts were pretreated at 873 K for 1 h in nitrogen flow, and the reaction temperature was 873 K. During reaction, the gas reactant contained 2.5 vol% propane, 5–30 vol% CO_2, and a balance of nitrogen. The feed and the reaction products were analyzed using an on-line gas chromatograph (Type GC-122, Shanghai) equipped with a 6-m packed column of Porapak Q and a flame ionization detector (FID). The permanent gas products, including N_2, CO, and CO_2, were analyzed on-line by another GC equipped with a TDX-01 column and a TCD detector. All carbon balances closed within 92–95%. The conversion and selectivity were calculated as follows:

$$C_3H_8 \text{ conversion} = \frac{C_3H_{8in} - C_3H_{8out}}{C_3H_{8in}} \times 100\%$$

$$C_3H_6 \text{ selectivity} = \frac{C_3H_{6out}}{C_3H_{8in} - C_3H_{8out}} \times 100\%$$

2.4. Temperature-programmed reaction of CO_2 with H_2

A temperature-programmed CO_2–H_2 test was carried out to investigate the activity of the In–Al mixed oxide catalysts for the RWGS reaction. The measurements were performed in a flow microreactor system. Prior to the experiment, a sample (100 mg) was outgassed in a flow of pure helium at 873 K for 30 min. Subsequently, the microreactor was cooled down to about 443 K. Reaction was performed using CO_2/H_2/He gas mixture with the ratio of 1:1:4 and total flow rate of 12 mL min^{-1}. The experiment was carried out with a linear heating rate of 10 K min^{-1} up to the final temperature of 973 K. The reactants and all possible products of reaction were continuously monitored by the QMS detector (Balzers OmniStar). The signal of the helium line served as the internal standard to compensate fluctuations of the operating pressure.

3. Results and discussion

3.1. Structural characterization and acid–base properties

Fig. 1 illustrates the diffractograms obtained for various In_2O_3–Al_2O_3 mixed oxides, along with those for bulk In_2O_3 and Al_2O_3 as references. The as-synthesized alumina was poorly crystallized, which is a common feature for γ-alumina [39], and even poorer crystalline signals of alumina are observed in the mixed oxide sam-

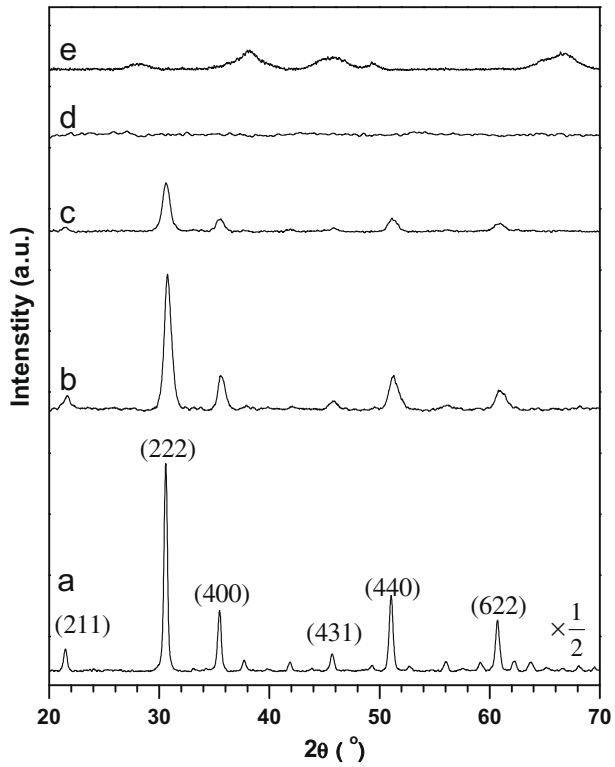

Fig. 1. XRD patterns of various In_2O_3–Al_2O_3 mixed oxides: (a) In_2O_3; (b) In–Al-40; (c) In–Al-20; (d) In–Al-10; (e) Al_2O_3.

ples. In contrast, the bulk In_2O_3 presents a well-crystallized phase. The peak intensities and their 2θ angles (30.6°, 35.6°, 51.3°, and 60.9°) have been identified as characteristic of the cubic structure of In_2O_3 (*c*-In_2O_3, JCPDS 6-0416). For all mixed oxide samples, except in the case of the In–Al-10 sample, the diffraction peaks corresponding to *c*-In_2O_3 phase are observed. The diffraction peaks corresponding to crystalline indium oxide phase of all In–Al–O samples are much weaker and broader than those of bulk In_2O_3, pointing to apparently higher component dispersion of the In_2O_3–Al_2O_3 composites with higher aluminum content. However, the positions of the diffraction lines for the mixed oxide samples were still the same as for the bulk indium oxide, indicating no Al substitution with In due to the relatively large difference of the atomic radii of In (0.79 Å) and Al (0.53 Å) atoms [40]. This fact, taking together with the significantly decreased crystallinities for Al_2O_3 and In_2O_3, suggests that the incorporation of alumina has not affected the crystalline structure of indium oxide but rendered better dispersions of both oxides.

Of all the mixed oxides investigated, the In–Al-10 catalyst shows the highest component dispersion, as reflected from the totally amorphous nature of this sample. This is also expected as a result of the highest specific surface area (195 $m^2\ g^{-1}$, see Table 1) of In–Al-10 when compared to other In_2O_3–Al_2O_3 samples. Surface acidity and basicity measurements by NH_3- and CO_2-TPD measurements (see Supplementary material, Tables S1 and S2 and Figs. S1 and S2) reveal an abundance of surface basic sites of medium strength and limited number of weak and medium strong acid sites in the bulk indium oxide. However, a much higher population of acidic sites than that of basic sites can be observed for the In–Al mixed oxide samples. It is worthwhile to note that the introduction of aluminum significantly modifies the acid–base distribution, increases both the overall acidity and basicity of indium oxide.

3.2. Redox behaviors and XPS studies

The reducibility of indium species in the In_2O_3–Al_2O_3 catalysts was investigated by TPR experiments. As shown in Fig. 2, the TPR profile of bulk In_2O_3 exhibits a single and broad peak centered at ca. 1000 K, attributable to the characteristic reduction of crystalline In_2O_3 to In^0 [34,35]. The hydrogen consumption is calculated to be 10.3 $mmol_{H2}\ g^{-1}$, corresponding to ca. 95% of the complete reduction of indium oxide. Distinct profile changes are identified for the reduction of In–Al mixed oxide samples, where two distinct reduction features are observed. The main reduction peak (β) ascribed to the reduction of crystalline phase In_2O_3 is shifted to a lower temperature of ca. 970 K in the In–Al mixed oxides, indicative of the presence of a In/Al interaction which facilitates the reduction of the dispersed In_2O_3. Gervasini et al. reported similar observations in their in-depth study on the nature of supported In_2O_3 catalysts for the SCR of NO_x and also compared the reduction of indium on various supports [38]. And it was noted that the dispersed InO_x species on the support are more reducible than the bulk In_2O_3. One can also see that with increasing alumina incorporation, the fraction of low temperature (LT) reduction peak (α) in the temperature range of 473–773 K, attributable to the reduction of dispersed indium oxide phase with smaller particles sizes to metallic In^0 species [34,35,38], is observed to be the highest for sample In–Al-10 when compared to other In_2O_3–Al_2O_3 samples (Table 1). This observation further confirms the presence of at least two types of In_2O_3 phase in the In_2O_3–Al_2O_3 samples, where crystallized indium oxide (β peak) and In_2O_3 phase highly dispersed on alumina (α peak) co-exist.

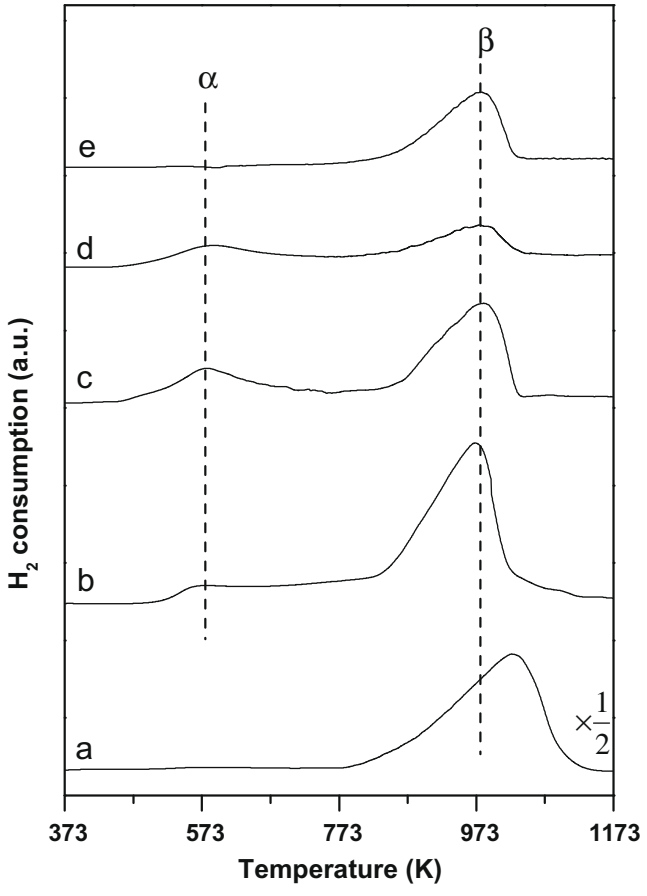

Fig. 2. TPR profiles of various In_2O_3–Al_2O_3 mixed oxides: (a) In_2O_3; (b) In–Al-40; (c) In–Al-20; (d) In–Al-10; (e) In–Al-20 pre-reduced by 5 vol% H_2/Ar at 773 K followed by CO_2 exposure at 873 K for 2 h.

Table 1
Physicochemical properties and characterization results of the mixed In_2O_3–Al_2O_3 oxides.

Sample	S_{BET} ($m^2\ g^{-1}$)	B.E. (eV) In $3d_{5/2}$	In/Al molar ratio		Peak temperature (K)		H_2 consumption (mmol g^{-1})		Percentage of In_2O_3 (α) [e] (%)
			Bulk[a]	Surface[b]	α[c]	β[d]	α[c]	β[d]	
In_2O_3	23	444.7	–	–	–	1026	0	10.3	0
In–Al-40	94	444.6	0.67	0.72	566	980	0.6	6	9.1
In–Al-20	174	444.5	0.25	0.27	573	976	1.6	3.2	33
In–Al-10	195	444.6	0.11	0.13	578	963	1.2	1.4	46
Al_2O_3	233	–	–	–	–	–	–	–	–

[a] The bulk In/Al molar ratio calculated from the ICP data.
[b] The surface In/Al molar ratio based on XPS analysis.
[c] The hydrogen consumption during 423–773 K calculated from the TPR results.
[d] The hydrogen consumption during 773–1073 K calculated from the TPR results.
[e] The percentage of In_2O_3 reduced during 423–773 K in TPR from the total amount of In_2O_3 reduced during the whole temperature range.

XPS experiments make it possible to determine not only the oxidation state, but also the In/Al ratio in the surface. These results are summarized in Table 1. In all cases, only one oxidation state was found, with binding energy for In $3\delta_{5/2}$ between 444.5 and 444.7 eV. These values are characteristic of In_2O_3 [41]. Considering that XPS is a surface sensitive technique, the In/Al ratio gives an idea of the component dispersion. The surface In/Al ratios are in line with the ICP data (see Table 1), confirming a high component dispersion of all mixed oxide samples. To gain further insight into the chemical state of indium species during reduction and the possible influence of CO_2 exposure upon metallic indium, XPS studies on In–Al-20 subjected to various atmospheric treatments were carried out (see Fig. 3 and Table 2). In the case of the fresh In–Al-20 sample (Fig. 3a), only bands assigned to In(III) species could be observed. After reduction treatment at 773 K (Fig. 3b), an additional feature signaling the formation of metallic In^0 (B.E. In $3d_{5/2}$ = 443.5 eV) species appeared. The In^0 accounted for 39.8 (atom%) of the total indium species based on deconvolution analysis (Table 2). This result agrees well with that (33%, in Table 1) of its likely precursor (highly dispersed In_2O_3) as estimated based on TPR results, implying all the existing In^0 derive exclusively from the highly dispersed In_2O_3 rather than bulk ones. TEM experiments have been carried out to observe a possible structure of the metallic In^0 particles. However, the identification of the small indium particles was unsuccessful, possibly due to the poor contrast between In^0 and metal oxides in the reduced sample. When this partially reduced sample is further subjected to an exposure of CO_2 at 873 K, no spectral variation could be observed (Fig. 3c). This indicates that the preformed metallic In^0 cannot be re-oxidized by CO_2 under reaction conditions, possibly due to the relatively weak oxidant potential of this molecule [16].

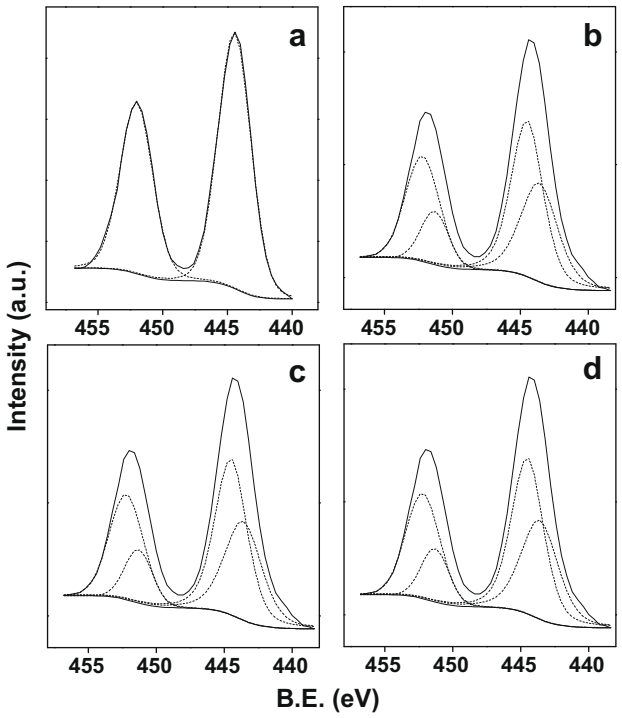

Fig. 3. XPS results of various In_2O_3–Al_2O_3 catalysts (a) fresh In–Al-20; (b) In–Al-20 pre-reduced by H_2/Ar at 773 K for 1 h; (c) In–Al-20 pre-reduced by H_2/Ar at 773 K for 1 h followed by exposure to a CO_2 stream (10 mL min^{-1}) at 873 K for 1 h; (d) In–Al-20 reacted for 8 h on stream at 873 K in the presence of CO_2 (Reaction conditions: $P(C_3H_8)$ = 2.5 kPa; $P(N_2)$ = 97.5 kPa; total flow rate: 10 mL min^{-1}).

3.3. Propane dehydrogenation activity

The dehydrogenation of propane to propylene over the In-containing materials along with Al_2O_3 in the absence of CO_2 was investigated at 873 K. The major product formed in the reaction is propylene, and the minor products are ethane, ethylene, and methane. The results, shown in Fig. 4, point to a marked composition effect on the catalytic performance of the In_2O_3–Al_2O_3 samples. Both simple oxides of In_2O_3 and Al_2O_3 demonstrated low propane conversion of <10%, which is fully in line with their inferior dehydrogenation activities as reported by Nakagawa et al. [21]. It is apparent moreover that all In-containing samples exhibited a very low selectivity toward propylene formation in the initial stage of the reaction, suggesting that an induction period is required to develop the active site. It is of interest to note that this performance evolution is quite different from all previously reported Cr_2O_3-,

Table 2
Summary of XPS studies.[a]

Sample	Sample description	B.E. for In $3d_{5/2}$ (eV)		B.E. for In $3d_{3/2}$ (eV)		Percentage of reduction (%)
		In^{3+}	In^0	In^{3+}	In^0	
A	fresh In–Al-20	444.5	–	452.2	–	–
B	Sample A reduced at 773 K for 1 h by H_2/Ar mixture[b]	444.5	443.5	452.2	451.2	39.8
C	Sample B subsequently treated with 10 mL min^{-1} CO_2 at 873 K for 1 h	444.5	443.5	452.2	451.2	39.7
D	In–Al-20 reacted for 8 h on stream in the absence of CO_2	444.5	443.5	452.2	451.2	39.4

[a] Note that the as-analyzed results could be in doubt as the measurement is not performed in situ.
[b] H_2/Ar molar ratio of 5/95 and a total flow of 40 mL min^{-1}.

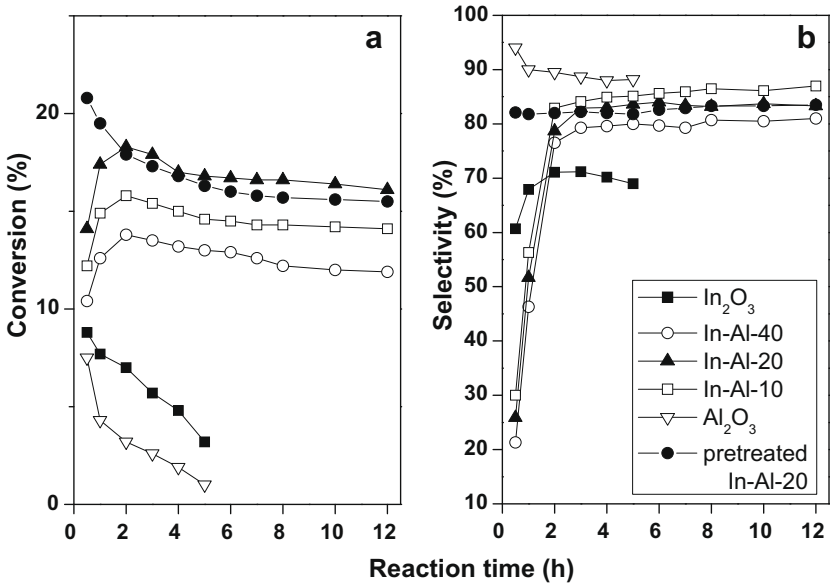

Fig. 4. Conversion of propane and selectivity to propylene for In_2O_3–Al_2O_3 mixed oxides. Reaction conditions: catalyst weight: 200 mg; $P(C_3H_8)$ = 2.5 kPa; $P(N_2)$ = 97.5 kPa; reaction temperature: 873 K; total flow rate: 10 mL min^{-1}. For comparison, the activity of a pre-reduced In–Al-20 sample is also included.

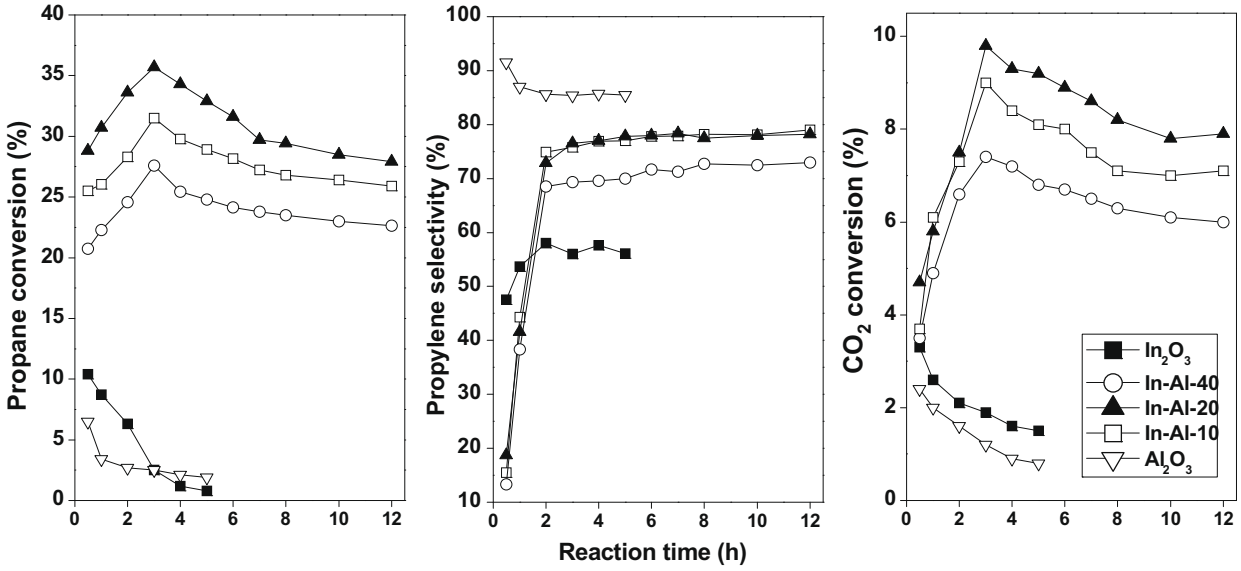

Fig. 5. Conversion of propane and selectivity to propylene for In_2O_3–Al_2O_3 mixed oxides at 873 K. Reaction conditions: catalyst weight: 200 mg; $P(C_3H_8)$ = 2.5 kPa; $P(CO_2)$ = 10 kPa; $P(N_2)$ = 87.5 kPa; total flow rate: 10 mL min^{-1}.

V_2O_5-, or Ga_2O_3-based catalyst systems during propane or ethane dehydrogenation [4,16,28,42,43]. After the induction period, significantly higher dehydrogenation activities that lead to selective conversion of propane with propylene yield in the range of 10–15% can be achieved for the In_2O_3–Al_2O_3 samples. The activity for the mixed oxide samples were shown to be exceptionally stable from 2 to 12 h, i.e. for In–Al-20 only a conversion loss by 2.2% was detected.

The dehydrogenation of propane was also run over the In_2O_3–Al_2O_3 mixed oxide samples as well as their simple oxide analogs at 873 K in the presence of CO_2, as was depicted in Fig. 5. The results show that the steady activity of the In_2O_3–Al_2O_3 catalysts in the presence of CO_2 is twice that in the absence of CO_2, although a slightly longer induction period (ca. 3 h) is required. It can be seen that all In_2O_3–Al_2O_3 samples led to a significant production of propylene with high selectivities (>70%) and appreciable "initial" steady conversions of propane ranging from ca. 27–37% at 3 h on stream. The "initial" steady conversions of propane decreased in the order In–Al-20 > In–Al-10 > In–Al-40. Note that the conversion of CO_2 in terms of reaction rate closely resembles to that of propane over all catalysts. The positive effect of CO_2 concentration on the propane dehydrogenation over In–Al-20 can be further seen from Fig. 6. All data were collected at the reaction time of 3 h. One can see that the rate of propylene formation remarkably increased together with that of CO formation with increasing the partial pressure of CO_2. On the other hand, the rate of H_2 formation showed no significant increase even with increasing the partial pressure of CO_2. All these facts indicate that the essential role of

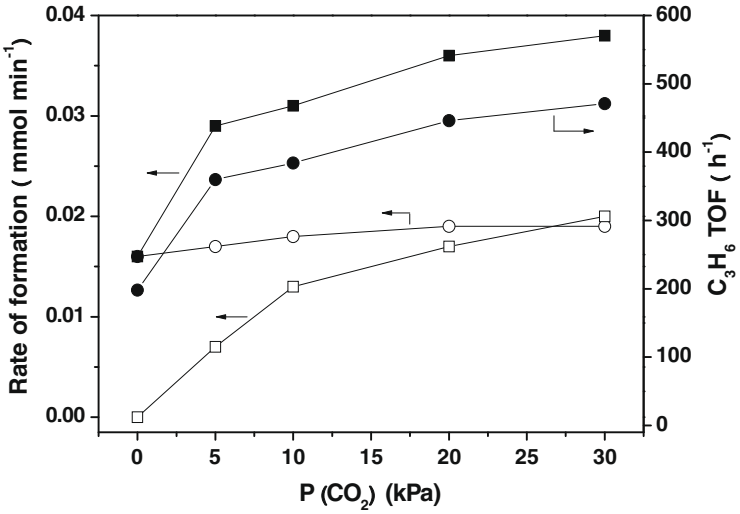

Fig. 6. Effect of partial pressure of CO_2 on the dehydrogenation of propane over In–Al-20 at 873 K. Rate of formation: (■) C_3H_6; (○) H_2; (□) CO; (●) TOF value for propylene formation estimated by assuming the In_2O_3 as quasi-sphere particles exposed with exclusively face (1 1 1) [40]. (Reaction conditions: $P(C_3H_8)$ = 2.5 kPa; total flow rate: 10 mL min^{-1}; balance gas: nitrogen.)

CO_2 is to promote the dehydrogenation process ($CH_3CH_2CH_3 \rightarrow CH_2=CHCH_3 + H_2$) by coupling the reaction of CO_2 with H_2 ($CO_2 + H_2 \rightarrow CO + H_2O$), which shifts the dehydrogenation equilibrium by consuming H_2. It is also interesting to remark that, owing to its intrinsic equilibrium nature, the overall RWGS reaction efficiency is not necessarily 100%, which can explain the evolution trend of the H_2 formation rate as a function of the CO_2 feed concentration as indicated in Fig. 6.

One of the biggest challenges in propane dehydrogenation with CO_2 is the deactivation of catalysts over a long period of reaction. To examine the likely long-term stability of the In–Al mixed oxide catalysts under the reaction conditions, an extended 30 h on-stream operation for dehydrogenation of propane in the presence of CO_2 was carried out on the In–Al-20 catalyst. As shown in Fig. 7, even after 30 h on-stream operation, a high conversion of propane up to 25.5% could still be maintained for In–Al-20. It is important to remark that this corresponds to only a 2.9% loss of its quasi steady activity at 8 h on stream. This is in sharp contrast to the previously reported supported Ga_2O_3-based system for PDH with CO_2, in which most of the gallia catalysts inclined to deactivate drastically in a few hours [29,30]. With high selectivity to propylene, such outstanding stability as to the indium-containing catalysts has never been reported before. This slowing of deactivation, when compared to the conventional Ga_2O_3-based catalysts, could be due to a moderate coke formation as a consequence of the apparently lower surface acidity of the supported indium-based materials. It is important, however, to point out that the In–Al-20 catalyst would deactivate rapidly within 12 h under reaction conditions with higher concentrated C_3H_8 feeds (for example, $P(C_3H_8)$ = 20 kPa; $P(CO_2)$ = 20 kPa; $P(N_2)$ = 60 kPa; total flow rate: 100 mL min^{-1}) (data not shown), possibly due to accelerated coke formation under more demanding conditions. Attempt was also made to regenerate In–Al-20 after 30 h on stream by re-calcination of the used catalyst in flowing air at 873 K for 4 h followed by sub-

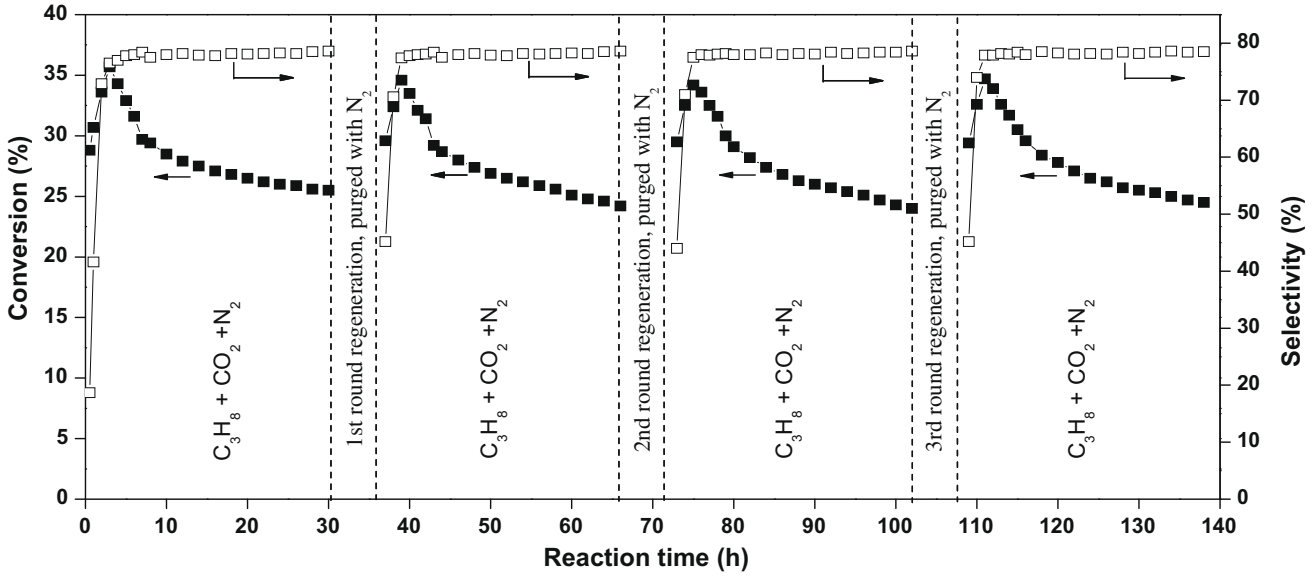

Fig. 7. The stability and regeneration of In–Al-20 at 873 K. Reaction conditions: catalyst weight: 200 mg; $P(C_3H_8)$ = 2.5 kPa; $P(CO_2)$ = 10 kPa; $P(N_2)$ = 87.5 kPa; total flow rate: 10 mL min^{-1}; flow rate of air or purging N_2: 40 mL min^{-1}.

sequent purge with N_2 for another 2 h (see Fig. 7). It is apparent that the original activity of In–Al-20 could be fully restored, with no noticeable deactivation being detected even after the third regeneration.

3.4. Active sites and structure–activity relationships

Previous investigations concerning the use of Cr_2O_3-, V_2O_5-, or Ga_2O_3-based catalysts for propane dehydrogenation in the presence of CO_2 have shown that, depending on the nature of the active sites, the reaction may proceed via two different reaction pathways. More specifically, it has been demonstrated that CO_2 improves the yield of propylene by two independent pathways. CO_2 can participate as an oxidizing agent in a Mars–van Krevelen-type redox cycle, in which the consumption and replenishment of the lattice surface oxygen species play a key role in the reaction process. Such simple redox mechanism has been proposed for the chromium, and vanadium oxide-based catalysts [16,42,43]. On the other hand, CO_2 can play a role in a removal of hydrogen produced in the dehydrogenation of propane by the reverse water–gas shift reaction. The reduction of partial pressure of hydrogen shifts the dehydrogenation equilibrium toward the propylene formation. Such promoting role of CO_2 was proposed to explain a high yield of propylene observed over the gallium oxide-based catalysts [7].

Given the high performance of the In_2O_3–Al_2O_3 catalyst for PDH, it is of interest to clarify the likely active species responsible for the observed dehydrogenation activity. It may be noted that the surface acidity or basicity (Tables S1 and S2) was not in line with the activity of different catalysts (Figs. 4 and 5), inferring that the surface acid–base nature is not the key factor governing the catalytic performance of the In_2O_3–Al_2O_3 samples. Taking into account the fact that the highly dispersed In_2O_3 is the widely accepted redox active site for NO_x removal during the SCR reaction [34,35], one might envisage that the present dehydrogenation reaction can proceed via a direct redox mechanism involving alternate reduction and oxidation of the surface InO_x sites. To testify this hypothesis, the TPR of the In–Al-20 sample was conducted after "reoxidation" of a hydrogen-pretreated In–Al-20 sample by CO_2. It should be mentioned here that the H_2-pre-treatment temperature at 773 K permits the reduction of the highly dispersed In_2O_3 but not the bulk one (see Fig. 2). As noted above, if the simple redox pathway is followed, one might expect that the reduced indium species would be readily re-oxidized by CO_2 atmosphere at 873 K. Nevertheless, the TPR profile as shown in Fig. 2e does not show any LT reduction feature in the temperature range of 473–773 K. This fact, together with the XPS analysis revealing that CO_2 is incapable of re-oxidizing In^0 to In_2O_3 (see Fig. 3c), strongly indicates that the direct redox mechanism is not applicable for the present In_2O_3-catalyzed dehydrogenation of propane in the presence of CO_2.

To further elucidate the active sites in the In_2O_3–Al_2O_3 system, the performance of the most active In–Al-20 catalyst for PDH in the absence of CO_2 was investigated after the pre-treatment with hydrogen (5% H_2/Ar at 773 K for 1 h). It is important to remark that the H_2-pre-treatment has a distinct influence on performance evolution of In–Al-20 at the initial stage of the reaction (Fig. 4), with essentially no influence on the steady-state activity of the catalyst. It is of interest to note that the H_2-pretreated In–Al-20 shows immediate high initial activity for PDH without experiencing the induction period as observed with the fresh In–Al-20 sample. Moreover, it must be pointed out that it is only after the induction period (ca. 2 h on stream) a steady conversion of propane with pronounced selectivity to propylene can be attained for fresh In–Al-20. All these facts, together with the XPS results showing a concomitant reduction of the dispersed In_2O_3 to the corresponding metallic In^0 species (see Fig. 5d), suggest that the surface-stabilized metallic In^0 nanoclusters that are generated in situ during the induction period could be the key active species for propane dehydrogenation. This speculation is further corroborated by the excellent correlation as identified for the relationship between the catalytic dehydrogenation activity and the amount of metallic In^0 species derived from the highly dispersed indium oxide species in the present In_2O_3–Al_2O_3 catalysts (Fig. 8).

Having established that In^0 species are the true active sites for simple dehydrogenation, it is also highly important to establish the possible role of indium in RWGS that may contribute to the positive effect of CO_2 for PDH. To this end, a temperature-programmed reaction of CO_2 with H_2 was conducted over the In_2O_3–Al_2O_3 samples as well as their simple oxide analogs, and the corresponding signals of CO were collected in Fig. 9a. It is evident that samples with higher fraction of bulk In_2O_3 exhibit higher yield of CO at identical temperatures, and the activity decreases in the order of In_2O_3 > In–Al-40 > In–Al-20 > In–Al-10 > Al_2O_3. This may suggest that bulk In_2O_3 is likely to be the active species for RWGS. To further confirm this assumption, In–Al-20 samples after pre-reduction at 773 and 1073 K were tested for RWGS, and the corresponding results were compared with that of the fresh In–Al-20 as shown in Fig. 9b. For the 773 K-reduced In–Al-20 (Fig. 9g), in which only highly dispersed In_2O_3 was converted to In^0, analogous activity to that of the fresh In–Al-20 is obtained, suggesting that the metallic In^0 may not be the key species for the RWGS reaction. For the 1073 K-reduced In–Al-20 (Fig. 9h), in which all indium was thoroughly reduced, dramatically lower CO yield relative to that of fresh In–Al-20 was observed. All these results clearly suggest that it is bulk In_2O_3 rather than metallic indium or highly dispersed In_2O_3 performed as the active phase for RWGS.

Finally, it is important to highlight that metallic indium, previously known to be a useful promoter in a number of formulated Pt–In/Al_2O_3 systems for commercial propane dehydrogenation [44,45], could become an interesting CO_2-mediated dehydrogenation catalyst when finely dispersed on a suitable support. More significantly, In_2O_3–Al_2O_3 was a far better catalyst in terms of catalytic

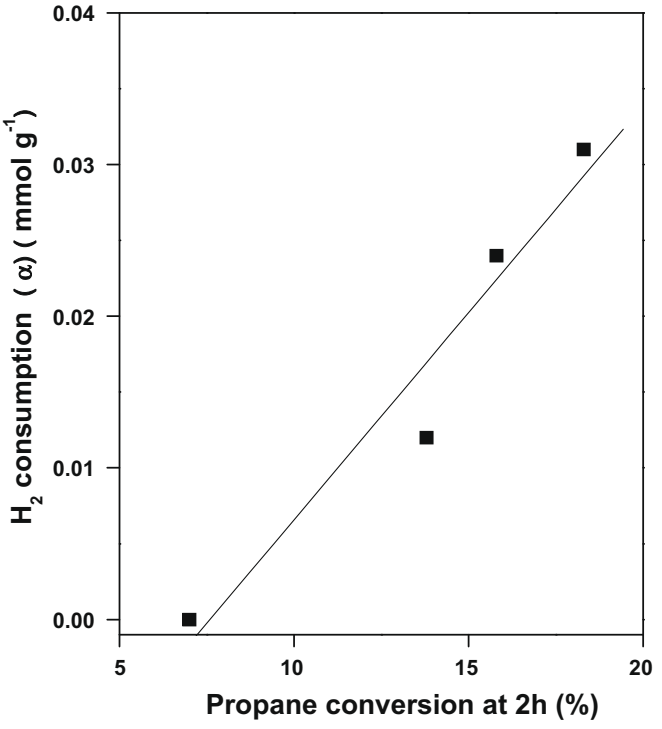

Fig. 8. Relationship between propane conversion at 2 h on stream in the absence of CO_2 and the corresponding LT hydrogen consumption (α) of the In_2O_3–Al_2O_3 catalysts.

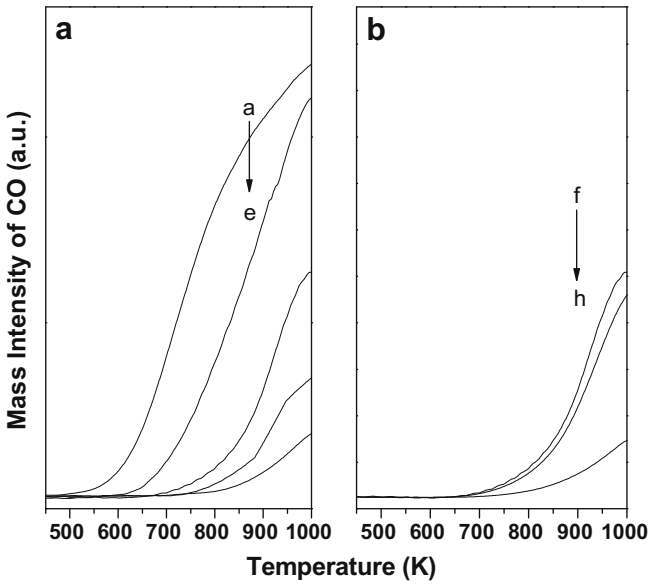

Fig. 9. Temperature-programmed CO_2–H_2 tests of CO_2 with H_2 for various In_2O_3–Al_2O_3 catalysts: (a) In_2O_3; (b) In–Al-40; (c) In–Al-20; (d) In–Al-10; (e) Al_2O_3 (f) fresh In–Al-20; (g) 773 K-H_2/Ar reduced In–Al-20; (h) 1073 K-H_2/Ar reduced In–Al-20.

stability for PDH with CO_2 compared to the most effective Ga_2O_3-based catalysts in the current literature [25,26]. Being different from all previously reported systems (for example, Cr_2O_3, V_2O_5, Ga_2O_3) [4,16,28,42,43], the results described in the present work show clearly a unique bifunctional character of the indium component in the In_2O_3–Al_2O_3 materials for propane dehydrogenation with CO_2. In this context, the overall reaction pathway can be envisaged to involve both metallic In species and the bulk In_2O_3 phase during the CO_2-mediated propane dehydrogenation process, i.e., the reaction proceeds via a simple metallic In^0-catalyzed dehydrogenation pathway facilitated by the RWGS reaction catalyzed by bulk In_2O_3. On the basis of the proposed main reaction pathway as described above, we can rationalize that a well balance of the metallic In species and the bulk In_2O_3 phase is indispensable for an efficient propane dehydrogenation over the In_2O_3–Al_2O_3 system.

4. Conclusions

The present work demonstrates the high potential of a new class of catalytic materials based on binary In–Al–O nanocomposites for the dehydrogenation of propane with CO_2. An optimum in the catalytic behavior was achieved for the catalyst containing 20% (atom.) In_2O_3, which can afford a propylene yield of 27.3% and maintain an exceptionally steady propane conversion of >24% during 30 h on stream. XRD and H_2-TPR characterizations suggest that the combination of indium and aluminum can result in significant modification in the bulk dispersion and surface redox properties of the In_2O_3 phase. The correlation of the catalytic activity and the TPR data unambiguously clarify that the creation and maintenance of surface metallic indium species in optimal surface concentration at the initial stage of the reaction are essential for achieving pronounced dehydrogenation activity. The promoting effect of CO_2 on the yield of propylene over the mixed oxide catalysts has been attributed to a facilitation of simple dehydrogenation by coupling with the bulk In_2O_3-catalyzed RWGS reaction.

Acknowledgments

This work was financially supported by the National Natural Science Foundation of China (20633030, 20721063, and 20873026), the National Basic Research Program of China (2009CB623506) the National High Technology Research and Development Program of China (2006AA03Z336), and Science and Technology Commission of Shanghai Municipality (08DZ2270500).

Appendix A. Supplementary material

Supplementary data associated with this article can be found, in the online version, at doi:10.1016/j.jcat.2010.03.007.

References

[1] F. Cavani, N. Ballarini, A. Cericola, Catal. Today 127 (2007) 113.
[2] G. Caeiro, R.H. Carvalho, X. Wang, M. Lemos, F. Lemos, M. Guisnet, F.R. Ribeiro, J. Mol. Catal. A 255 (2006) 131.
[3] P. Michorczyk, J. Ogonowski, Appl. Catal. A 251 (2003) 425.
[4] M. Saito, S. Watanabe, I. Takahara, M. Inaba, K. Murata, Catal. Lett. 89 (2003) 213.
[5] M.M. Bhasin, J.H. McCain, B.V. Vora, T. Imai, P.R. Pujado, Appl. Catal. A 221 (2001) 397.
[6] K. Nakagawa, C. Kajita, Y. Ide, M. Okamura, S. Kato, H. Kasuya, N. Ikenaga, T. Kobayashi, T. Suzuki, Catal. Lett. 64 (2000) 215.
[7] K. Nakagawa, C. Kajita, K. Okumura, N.-O. Ikenaga, M. Nishitani-Gamo, T. Ando, T. Kobayashi, T. Suzuki, J. Catal. 203 (2001) 87.
[8] J. Gascon, C. Tellez, J. Herguido, M. Menendez, Appl. Catal. A 248 (2003) 105.
[9] M. Larsson, M. Hulten, E.A. Blekkan, B. Andersson, J. Catal. 164 (1996) 44.
[10] M.M. Bettahar, G. Costentin, L. Savary, J.C. Lavalley, Appl. Catal. A 145 (1996) 1.
[11] E.A. Mamedov, V.C. Corberan, Appl. Catal. A 127 (1995) 1.
[12] Y.M. Liu, Y. Cao, S.R. Yan, W.L. Dai, K.N. Fan, Catal. Lett. 88 (2003) 61.
[13] Y.M. Liu, Y. Cao, N. Yi, W.L. Feng, W.L. Dai, S.R. Yan, H.Y. He, K.N. Fan, J. Catal. 224 (2004) 417.
[14] Y.M. Liu, Y. Cao, K.K. Zhu, S.R. Yan, W.L. Dai, H.Y. He, K.N. Fan, Chem. Commun. (2002) 2832.
[15] K. Nakagawa, C. Kajita, N. Ikenaga, M. Nishitani-Gamo, T. Ando, T. Suzuki, Catal. Today 84 (2003) 149.
[16] K. Takehira, Y. Ohishi, T. Shishido, T. Kawabata, K. Takaki, Q.H. Zhang, Y. Wang, J. Catal. 224 (2004) 404.
[17] P. Kustrowski, M. Zbroja, R. Dziembaj, H. Papp, Catal. Lett. 80 (2002) 1.
[18] K. Nowinska, A. Waclaw, A. Izbinska, Appl. Catal. A 243 (2003) 225.
[19] E.V. Kondratenko, M. Cherian, M. Baerns, D. Su, R. Schlogl, X. Wang, I.E. Wachs, J. Catal. 234 (2005) 131.
[20] S.B. Wang, Z.H. Zhu, Energy Fuels 18 (2004) 1126.
[21] K. Nakagawa, M. Okamura, N. Ikenaga, T. Suzuki, T. Kobayashi, Chem. Commun. (1998) 1025.
[22] Y. Wang, Y. Ohishi, T. Shishido, Q.H. Zhang, W. Yang, Q. Guo, H.L. Wan, K. Takehira, J. Catal. 220 (2003) 347.
[23] I. Takahara, W.C. Chang, N. Mimura, M. Saito, Catal. Today 45 (1998) 55.
[24] H. Shimada, T. Akazawa, N. Ikenaga, T. Suzuki, Appl. Catal. A 168 (1998) 243.
[25] M. Chen, J. Xu, Y.M. Liu, Y. Cao, H.Y. He, J.H. Zhuang, K.N. Fan, Catal. Lett. 124 (2008) 369.
[26] M. Chen, J. Xu, F.Z. Su, Y.M. Liu, Y. Cao, H.Y. He, K.N. Fan, J. Catal. 256 (2008) 293.
[27] D.Y. Hong, J.S. Chang, J.H. Lee, V.P. Vislovskiy, S.H. Jhung, S.E. Park, Y.H. Park, Catal. Today 112 (2006) 86.
[28] H.Y. Li, Y.H. Yue, C.K. Miao, Z.K. Xie, W.M. Hua, Z. Gao, Catal. Commun. 8 (2007) 1317.
[29] B.J. Xu, B. Zheng, W.M. Hua, Y.H. Yue, Z. Gao, J. Catal. 239 (2006) 470.
[30] B. Zheng, W.M. Hua, Y.H. Yue, Z. Gao, J. Catal. 232 (2005) 143.
[31] M.P. Lobera, C. Téllez, J. Herguido, M. Menéndez, Appl. Catal. A 349 (2008) 156.
[32] M.S. Kumar, N. Hammer, M. Ronning, A. Holmen, D. Chen, J.C. Walmsley, G. Oye, J. Catal. 261 (2009) 116.
[33] M.S. Kumar, D. Chen, A. Holmen, J.C. Walmsley, Catal. Today 142 (2009) 17.
[34] J.A. Perdigon-Melon, A. Gervasini, A. Auroux, J. Catal. 234 (2005) 421.
[35] P.W. Park, C.S. Ragle, C.L. Boyer, M.L. Balmer, M. Engelhard, D. McCready, J. Catal. 210 (2002) 97.
[36] T. Maunula, Y. Kintaichi, M. Haneda, H. Hamada, Catal. Lett. 61 (1999) 121.
[37] M. Haneda, Y. Kintaichi, H. Hamada, Catal. Lett. 55 (1998) 47.
[38] A. Gervasini, J.A. Perdigon-Melon, C. Guimon, A. Auroux, J. Phys. Chem. B 110 (2006) 240.
[39] C.O. Arean, M.R. Delgado, V. Montouillout, D. Massiot, Z. Anorg. Allg. Chem. 631 (2005) 2121.
[40] C.T. Prewitt, R.D. Shannon, D.B. Rogers, A.W. Sleight, Inorg. Chem. 8 (1969) 1985.
[41] A.W.C. Lin, N.R. Armstrong, T. Kuwana, Anal. Chem. 49 (1977) 1228.
[42] Y. Ohishi, T. Kawabata, T. Shishido, K. Takaki, Q.H. Zhang, Y. Wang, K. Takehira, J. Mol. Catal. A 230 (2005) 49.
[43] P. Michorczyk, K. Gora-Marek, J. Ogonowski, Catal. Lett. 109 (2006) 195.
[44] F.A. Marchesini, S. Irusta, C. Querini, E. Mir, Catal. Commun. 9 (2008) 1021.
[45] F.B. Passos, M. Schmal, M.A. Vannice, J. Catal. 160 (1996) 106.